Proceedings of the
44th IEEE Conference on Decision and Control, and
the European Control Conference 2005
Seville, Spain, December 12-15, 2005

Reachability Analysis of Continuous-Time Piecewise Linear Systems

Abdullah O. Hamadeh, Jorge M. Gonçalves
Department of Engineering
University of Cambridge
Cambridge CB2 1PZ, UK
aoh21@cam.ac.uk, jmg77@cam.ac.uk

Abstract— **This paper presents a new approach to the reachability problem for a class of hybrid systems called Piecewise Linear Systems (PLS). The principal tool used is the impact map between switching surfaces. The method consists of specifying a ellipsoidal set on the initial switching surface and finding upper- and lower-bound estimates of the possible reach sets using tools such as the S-procedure to set up linear matrix inequalities, of which numerical solutions are then computed.**

I. Introduction

Systems that consist of interactions between discrete and continuous dynamics are termed hybrid systems, and these represent a general class of systems widely modelled today such as digitally-controlled continuous systems, the cell cycle, walking robots, systems with hysteresis and saturating systems.

Knowledge of reachability gives us a range of important details for a particular system such as:

- Safety: Will the system ever go into unsafe regions?
- Liveness: Will the system reach a 'good' state?
- Stability: Will the system remain in an invariant set about an equilibrium point?
- Performance: Will the system remain in an invariant set about a specific reference point?
- Tracking: Can we identify what states will be reached in order to aid tracking of the system?

In this paper we analyse a particular class of hybrid systems, namely those that are piecewise linear (PLS). These are characterised by a finite number of linear systems covering separate cells in the state-space, together with a set of rules for switching among the various models.

In the literature, much of the reachability analysis is of systems with uncertainty, as in [1]. There have been numerous papers, such as [2], [3], that have dealt with reachability in discrete time systems. Little work on reachability in continuous-time PLS has been done, however.

In [4] a new approach was introduced that globally analysed PLS, consisting of finding Lyapunov functions on the switching surfaces to prove that Poincaré type maps associated with the system were contracting. These generalised Poincaré maps, or impact maps, are defined from one switching surface to another. This work introduced a new technique that involved expressing the impact map as a linear transformation parameterised by the switching time. This led to the ability to numerically solve sets of linear matrix inequalities (LMIs) to find surface Lyapunov functions.

The main technique in this paper involves setting up constraints relating the start and reach sets. From these, we can derive LMIs that are functions of the switching times and we obtain approximations of the reach set by solving these inequalities. This paper begins by briefly describing PLS and impact maps. The next step is to find the range of switching times associated with a particular initial set, which will be needed in solving the LMIs. We then discuss various approaches to computing upper and lower bounds on the reach set, and then end with a two examples of this technique and ideas for Future Work.

II. Piecewise Linear Systems

In Piecewise Linear Systems the state-space is divided into M different regions. In each region, the system is linear (see Figure 1). The over-all system obeys:

$$\dot{x} = A_\alpha x + B_\alpha, \alpha \in \{1 \ldots M\}$$

Switches occur at switching surfaces consisting of hyperplanes of dimension *n-1*, given by points $S_j = \{x \in \mathbb{R}^n | C_j x = d_j\}$ for some row vector C_j and scalar d_j, $j = \{1 \ldots N\}$.

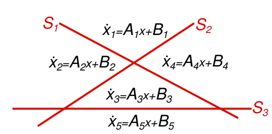

Fig. 1. A piecewise linear system is composed of multiple cells separated by switching surfaces.

III. Impact Maps

Consider two switching surfaces S_0, S_1 such that:

$$S_0 = \{x \in \mathbb{R}^n | C_0 x = d_0\}$$
$$S_1 = \{x \in \mathbb{R}^n | C_1 x = d_1\} \quad (1)$$

We can define a set $U_d \subset S_0$ of points where any trajectory starting in U_d will next switch at S_1. We can also call the set in S_1 which those points first reach U_a. Next, consider a general vector $\Delta_0 \in S_0$ ($\Delta_1 \in S_1$) with a reference origin at $x_0^* \in S_0$ ($x_1^* \in S_1$). We can now define a point $x_0 \in S_0$ ($x_1 \in S_1$) as $x_0 = x_0^* + \Delta_0$ ($x_1 = x_1^* + \Delta_1$), as is illustrated in Figure 2.

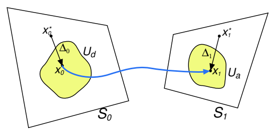

Fig. 2. Point x_0^* (x_1^*) is a reference point in S_0 (S_1). We can therefore write any point $x_0 \in S_0$ ($x_1 \in S_1$) as $x_0 = x_0^* + \Delta_0$ ($x_1 = x_1^* + \Delta_1$). U_d is the departure set of points in S_0 that next switch at S_1, and U_a is their arrival set on S_1.

The dynamics in between S_0 and S_1 are given by:

$$\dot{x}(t) = Ax(t) + B \tag{2}$$

With initial condition $x_0 \in S_0$, integrating (2) gives:

$$x(t) = e^{At}x_0 + \int_0^t e^{A(t-\tau)}Bd\tau \tag{3}$$

Assume the first switch is at $x_1 \in S_1$ with a switching time $t = t_s$, i.e. $x_1 = x(t_s)$. Let $x_0^* \in S_0$ and $x_1^* \in S_1$. Substituting $x_0 = x_0^* + \Delta_0$ and $x_1 = x_1^* + \Delta_1$ into (3) gives $\Delta_1 = e^{At}\Delta_0 + x_0^*(t) - x_1^*$, where $x_0^*(t)$ is the trajectory of (3) with initial condition x_0^*. Note that if A is invertible:

$$x_0^*(t) = e^{At}(x_0^* + A^{-1}B) - A^{-1}B$$

The impact map from Δ_0 to Δ_1 is then given by [4]:

$$\Delta_1 = H(t)\Delta_0 \tag{4}$$

where:

$$H(t) = e^{At} + (x_0^*(t) - x_1^*)w(t) \tag{5}$$

and

$$w(t)\Delta_0 = \frac{C_1 e^{At}\Delta_0}{d_1 - C_1 x_0^*(t)} = 1 \tag{6}$$

The function $H(t)$ defines the impact map from S_0 to S_1. At first, this mapping appears to be non-linear. However, if we fix the switching time, we notice that $H(t)$ becomes a linear mapping, thus simplifying the analysis. This idea will be used throughout this thesis to analyse mappings between switching surfaces.

In general, for an n-dimensional system, a switching surface S_j is an $n-1$-dimensional hyperplane where we can write:

$$C_j\Delta_j = 0 \tag{7}$$

since column vector Δ_j lies on the hyperplane S_j and C_j is a row vector perpendicular to S_j. In fact, we can write Δ_j as $\Delta_j = \Pi_j\delta_j$, where $\Pi_j \in C_j^\perp$, the orthogonal complement of C_j. Π_j is therefore a matrix composed of the the maximal number of normalised column vectors orthogonal to C_j. Since the switching surface is of dimension $n-1$, the width of matrix Π_j and the dimension of vector δ_j are $n-1$.

We can therefore think of (4) as the mapping of two $n-1$ dimensional vectors on the switching surface, δ_0 to δ_1:

$$\delta_1 = \bar{H}(t)\delta_0 \tag{8}$$

where $\bar{H}(t) = \Pi_1^T H(t)\Pi_0$, since $\Pi_1^T\Pi_1 = I$.

IV. Bounds On Switching Times

When mapping a set of points from $U_d \subset S_0$ to $U_a \subset S_1$, each point will have a switching time associated with it. Since impact maps are parameterised by the switching time, we need to find bounds on the switching times of initial sets in U_d.

In [4] we saw that the set of points on S_0 having the same switching time is always a convex subset of a linear manifold of dimension $n-2$. This follows from the fact that any point on S_0 must satisfy two linear equations on Δ_0: (6) and (7). This is illustrated in Figure 3.

For example, if the initial set were an ellipse, then by finding subsets of constant switching time that are tangent to the ellipse, we find the range of switching times $\mathcal{T}$ of points in the ellipse, as shown in Figure 4.

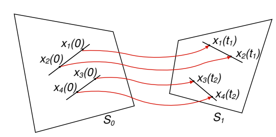

Fig. 3. Lines are subsets of the same switching time.

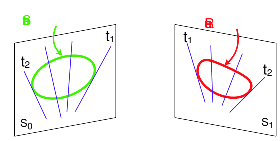

Fig. 4. The range of switching times $\mathcal{T}$ is [t_1,t_2].

V. Minimum Upper Bound Computation

We wish to find the lowest upper bound on the reachable set when starting in some initial set on the switching surface S_0. If we wish to ensure that the system will not enter any unsafe regions, we would use this upper bound to compute the trajectories in the cell and we would need to ensure that the trajectories emanating from this upper bound do not enter unsafe regions. We begin by defining an ellipsoid containing the initial set. Therefore, we can write that for any vector $\Delta_0 = \Pi_0\delta_0$, centered on x_0^*, in this initial set:

$$\left\|P_0^{\frac{1}{2}}\delta_0\right\|^2 = \delta_0^T P_0 \delta_0 \le \Gamma_0^2$$

where $P_0 \ge 0$ is the matrix defining the ellipsoid on the switching surface. From now we will use the shorthand notation $\left\|P_j^{\frac{1}{2}}\delta_j\right\|^2 \equiv \left\|\delta_j\right\|_{P_j}^2$.

A vector $\delta_0 \in S_0$ will map onto a vector $\delta_1 \in S_1$. Now let the reach set be similarly bounded by an ellipsoid given by:

$$\|\delta_1\|^2_{P_1^u} \leq \Gamma_1^2$$

where $P_1^u \geq 0$ is a matrix defining the ellipsoid, the superscript u denoting this ellipsoid as an upper bound. Without loss of generality, let $\Gamma_0 = \Gamma_1 = 1$. This can be done by scaling P_j by $\frac{1}{\Gamma_j^2}$ to give $\bar{P}_j$. Therefore the problem we want to solve is to find the smallest ellipsoid in S_1 such that:

$$1 - \|\delta_0\|^2_{\bar{P}_0} \geq 0 \Rightarrow 1 - \|\delta_1\|^2_{\bar{P}_1^u} \geq 0 \quad (9)$$

Figure 5 illustrates these constraints. Now we want a single relation that says that non-negativity of of the left side of 9 implies non-negativity of the right. We therefore apply the S-procedure (see [5] for a discussion of the S-procedure):

$$\left(1 - \|\delta_1\|^2_{\bar{P}_1^u}\right) - \tau_1 \left(1 - \|\delta_0\|^2_{\bar{P}_0}\right) \geq 0 \quad (10)$$

where $\tau_1 \geq 0$. The point of using the S-procedure here is to find a condition such that non-negativity of $1 - \|\delta_0\|^2_{\bar{P}_0}$ implies non-negativity of $1 - \|\delta_1\|^2_{\bar{P}_1^u}$. In other words, if δ_0 lies within the ellipsoid on the departure switching surface, the vector δ_1 lies within the ellipsoid on arrival switching surface. We wish to find the smallest ellipsoid making up the reach set. For this, we first need to find the limits on τ_1 in (10). From (8) we know that as $\|\delta_0\| \to 0$, (10) approaches a limit where $\tau_1 \leq 1$:

The tightest bound, and therefore the smallest upper bound on the reach set, is obtained when $\tau_1 = 1$. Substituting (8) and this value of τ_1 into (10) yields a linear matrix inequality (LMI) that we need to solve for $\bar{P}_1^u \geq 0$ given by:

$$\delta_0^T \left(\bar{P}_0 - \bar{H}^T(t)\bar{P}_1^u \bar{H}(t)\right) \delta_0 \geq 0 \quad (11)$$

If we define $Q_1(t)$ as:

$$Q_1(t) = \left(\bar{P}_0 - \bar{H}^T(t)\bar{P}_1^u \bar{H}(t)\right) \quad (12)$$

then to find the minimum upper bound we need to find a $\bar{P}_1^u \geq 0$ such that $Q_1(t) \geq 0$, $\forall t \in \mathcal{T}$.

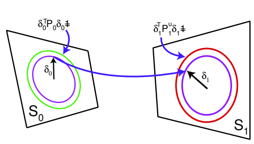

Fig. 5. Upper bound approximations on initial and reach sets for a 3D system.

VI. Maximum Lower Bound Computation

We now consider a reverse approach to the reachability problem compared to one proposed above. We now wish to find the set that we know we can reach given an initial set on S_0. We begin by specifying a candidate ellipsoid on S_1 and call this $\delta_1^T \bar{P}_1^l \delta_1 = 1$, where $P_1^l \geq 0$ and the superscript l denotes this as a lower bound. We then map this ellipsoid onto the initial switching surface S_0 to see if it maps entirely into the initial ellipsoid given by $\delta_0^T \bar{P}_0 \delta_0 = 1$. If it does then we have a lower bound on the reach set. In this case we say that if we start in a given ellipsoid $\delta_0^T \bar{P}_0 \delta_0 = 1$ on S_0, then we are certain that we can reach an ellipsoid $\delta_1^T \bar{P}_1^l \delta_1 = 1$ on S_1, though $\delta_0^T \bar{P}_0 \delta_0 = 1$ will then contain points that can reach beyond the limits of $\delta_1^T \bar{P}_1^l \delta_1 = 1$ as well. If we seek to maximise the reachable regions of the system we would therefore need to maximise the size of the ellipsoid $\delta_1^T \bar{P}_1^l \delta_1 = 1$.

We start as in section V, by first scaling P_j by $\frac{1}{\Gamma_j^2}$ to give $\bar{P}_j$ and then writing:

$$1 - \|\delta_1\|^2_{\bar{P}_1^l} \geq 0 \Rightarrow 1 - \|\delta_0\|^2_{\bar{P}_0} \geq 0$$

That is, if the point reached is in $\delta_1^T \bar{P}_1^l \delta_1 = 1$, then the initial state was within $\delta_0^T \bar{P}_0 \delta_0 = 1$. Applying the S-procedure:

$$\left(1 - \|\delta_0\|^2_{\bar{P}_0}\right) - \tau_2 \left(1 - \|\delta_1\|^2_{\bar{P}_1^l}\right) \geq 0 \quad (13)$$

In analogy with (4), we will now define a 'reverse' impact map, $J(t)$ (see Appendix I) which maps $\Delta_1 \in S_1$ onto $\Delta_0 \in S_0$:

$$\Delta_0 = J(t)\Delta_1 \quad (14)$$

If we let $\bar{J}(t) = \Pi_0^T J(t) \Pi_1$ as in (8) we can write (14) as:

$$\delta_0 = \bar{J}(t)\delta_1 \quad (15)$$

As $\|\delta_0\| \to 0$, (13) approaches the limit: $\tau_2 \leq 1$. The tightest bound, giving the greatest lower bound on the reach set, is obtained when $\tau_2 = 1$.
Substituting (14) and $\tau_2 = 1$ back into (13):

$$\delta_1^T \left(\bar{P}_1^l - \bar{J}^T(t)\bar{P}_0 \bar{J}(t)\right) \delta_1 \geq 0 \quad (16)$$

This LMI can then be solved numerically by finding a $\bar{P}_0 \geq 0$ that gives a $Q_2(t) \geq 0 \forall t$, where:

$$Q_2(t) = \left(\bar{P}_1^l - \bar{J}^T(t)\bar{P}_0 \bar{J}(t)\right) \geq 0 \quad (17)$$

Note that (17) is a different LMI for each switching time $t \in \mathcal{T}$. Therefore, to compute the maximum lower bound, we must solve (17) for the matrix $\bar{P}_1^l$ that gives the largest ellipsoid $\delta_1^T \bar{P}_1^l \delta_1 = 1$ while ensuring that $Q_2(t) \geq 0$, $\forall t \in \mathcal{T}$.

With this approach, we specify a reach set in S_1, and then find the starting set in S_0. To find the range of switching times given the reach set, we use a similar approach to that detailed in section IV, only this time, we cannot use the relation in (6) as it operates on Δ_0. We can write an expression $v(t)$, similar to $w(t)$ in (6) that operates on Δ_1, if we are given the reach set (see Appendix I):

$$v(t)\Delta_1 = 1 \quad (18)$$

Note that if the switching time is fixed, (18) is a linear equation. Also, we can write, for $\Delta_1 \in S_1$ that $C_1\Delta_1 = 0$. Therefore, we have two linear equations that we can use to characterise sets of points in S_1 with the same switching time, and therefore each such set of points is again of dimension $n-2$.

We apply this method after the one described in section V. We began in the previous section by defining a set $\Gamma_0 \in S_0$, computing the nominal reach point x_1^* and the reach set $\Gamma_1 \in S_1$. Now consider a proper subset of $\Gamma_1 \in S_1$, centered on x_1^* and call this new subset Γ_2. Now this new subset becomes the new 'start set' and we use the reverse impact map, $\bar{J}(t)$, to compute the new 'reach set', say $\Gamma_3 \in S_0$. Now, if $\Gamma_3 \subset \Gamma_0$, we know that every point in $\Gamma_2 \in S_1$ can be reached from $\Gamma_3 \in S_0$, and so $\Gamma_2 \in S_1$ is a lower bound on the reach set. Therefore we gradually increase $\Gamma_2 \in S_1$ until $\Gamma_3 \nsubseteq \Gamma_0$. At that point we would know that Γ_2 is a maximum lower bound on the reach set.

VII. Continuity and Tangential Trajectories

When we consider the mapping of a set of points from S_0 to S_1 we need to ensure that the map is continuous in the domain of the impact map. Consider, however, two trajectories in a PLS that start close to each other on S_0, as in Figure 6. One of the trajectories is tangential to S_1 and does not switch, whilst the other one does. In this case, the set in which these two trajectories start is non-continuous, as the distance between the two paths becomes unbounded with time.

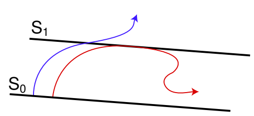

Fig. 6. A transversal trajectory (blue) and a tangential one (red).

From [6], at the switching time of trajectory $x(t)$, $t = t_s$, we have $C_1 x(t) = C_1 x_1^* + C_1 \Delta_1 = d_1$. Also, the distance between the switching surface and the trajectory at time t is $C_1 x(t) - d_1$. At the switching time, this distance is zero, and therefore tangential trajectories are those where:

$$\left. \frac{d(C_1 x(t) - d_1)}{dt} \right|_{t=t_s} = 0 \tag{19}$$

Therefore in an initial set on S_0 that maps onto S_1, to ensure that there are no trajectories emanating from this set that are tangential to S_1, we must ensure that the hyperplanes of (19) do not intersect with the set of points on S_0. This ensures that the initial set is continuous.

In this analysis, all trajectories starting from points in a given start set on S_0 must next switch on the same switching surface S_1. Thus, the initial set may need to be reduced to guarantee the domain of S_0 has no points that switch before reaching S_1, as in Figure 7. If the switching surfaces form convex cells, which are the simplest and most common cases, the procedure explained above can be applied to derive an equality similar to (19) for each hyperplane that is a boundary of the cell. The case of non-convex cells is still under investigation.

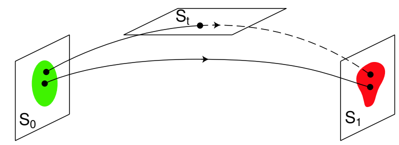

Fig. 7. Trajectories may switch at S_t before reaching S_1.

VIII. Two-Dimensional Example

We have a LTI system given by:

$$\begin{bmatrix} \dot{x}_1 \\ \dot{x}_2 \end{bmatrix} = \begin{bmatrix} 1 & 3 \\ 0 & 1 \end{bmatrix} \begin{bmatrix} x_1 \\ x_2 \end{bmatrix} + \begin{bmatrix} 1 & 0 \\ 0 & 1 \end{bmatrix} \begin{bmatrix} u_1 \\ u_2 \end{bmatrix} \tag{20}$$

This LTI system is part of an autonomous system where the outputs y_1 and y_2 are each fed into a saturater with outputs u_1 and u_2 respectively (see Figure 8). Each saturater has three linear regions of operation, and so the state-space is divided into nine cells by four switching surfaces. The outputs are functions of the state and are given by:

$$\begin{bmatrix} y_1 \\ y_2 \end{bmatrix} = \begin{bmatrix} C_1 \\ C_2 \end{bmatrix} \begin{bmatrix} x_1 \\ x_2 \end{bmatrix} = \begin{bmatrix} 1 & 1 \\ -1 & 1 \end{bmatrix} \begin{bmatrix} x_1 \\ x_2 \end{bmatrix}$$

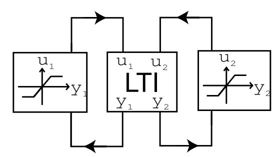

Fig. 8. Outputs y_1 and y_2 are each fed into a saturater with outputs u_1 and u_2 respectively.

The four switching surfaces are given by $C_m x = d_n$ for $m, n = 1, 2$, with $d_1 = 1$ and $d_2 = -1$. Now consider a nominal trajectory starting at $x_0^* = [\ 2 \quad -1\ ]^T$, which is on $C_1 x = d_1$. The trajectory will enter a cell where the dynamics of the system are:

$$\begin{bmatrix} \dot{x}_1 \\ \dot{x}_2 \end{bmatrix} = \begin{bmatrix} 2 & 4 \\ 0 & 1 \end{bmatrix} \begin{bmatrix} x_1 \\ x_2 \end{bmatrix} + \begin{bmatrix} 0 \\ -1 \end{bmatrix} \tag{21}$$

Here, the switching surfaces are lines, and so instead of the ellipsoid, we consider a segment of the line around x_0^* that contains all vectors $\Delta_0 = \Pi_0 \delta_0 = \frac{1}{\sqrt{2}}[\ 1 \quad -1\ ]^T \delta_0$. The nominal trajectory next switches at $x_1^* = [\ 1 \quad -2\ ]^T$, which is on $C_1 x = d_2$. If there is now an uncertainty in the initial state given by Γ_0, we can define all points up to Γ_0 away from x_0 along the switching surface to be the initial set. Here, $\Gamma_0 = 0.75\sqrt{2} \approx 1.06$ and we now wish to find an upper and lower bound on the reach set Γ_1 on $C_1 x = d_2$.

Figure 9 shows the initial points and the points that are reached in green and red respectively, computed numerically. Now applying the method proposed in sections V and VI, we need to find the values of Γ_1 where the functions $Q_1(t)$

and $Q_2(t)$ (from equations (12) and (17) in previous chapter) become positive for all switching times. Note that since this is a 2D case we need not examine any eigenvalues of $Q_1(t)$ and $Q_2(t)$ to ensure that they are positive semi-definite, as these are scalar functions. We also set $P_0 = P_1 = 1$ and multiply through by Γ_0^2.

Figure 10 shows the functions $Q_1(t)$ and $Q_2(t)$ against switching time. When Γ_1 is equal to the upper bound shown in Figure 9 the function $Q_1(t)$ just becomes positive for all switching times. At the point where Γ_1 just becomes equal to the lower bound shown in Figure 9, $Q_2(t)$ just becomes positive for all switching times.

Table I compares the sizes of the reach sets Γ_1 obtained both numerically and with the proposed method. It can be seen that the results obtained are almost exact and the discrepancy can be attributed to numerical error for this two dimensional example. Subsequent mappings also show exact agreement and the upper and lower bounds for these mappings are shown in Figures 11(a) and 11(b).

	Γ_1: Numerically	Γ_1: Proposed Method
Upper Bound	0.8910	0.8910
Lower Bound	0.4544	0.4545

TABLE I

SIZES OF REACH SETS

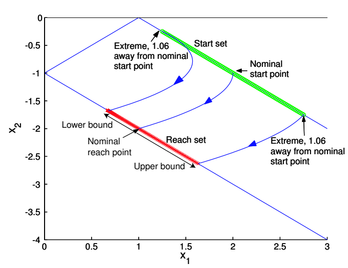

Fig. 9. Start and reach points with $\Gamma_0 = 1.06$. The upper bound reach set is $\Gamma_1 = 0.89$ and the lower bound reach set is $\Gamma_1 = 0.45$.

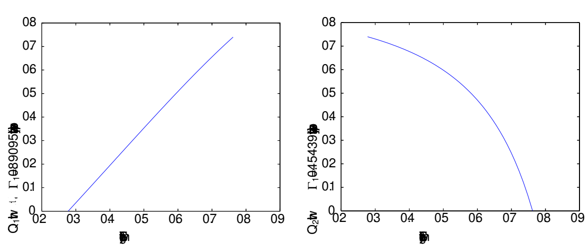

(a) 1^{st} map - Upper bound (b) 1^{st} map - Lower bound

Fig. 10. Values of functions $Q_1(t)$ and $Q_2(t)$

IX. Three Dimensional Example

For an example of this method at work for a three-dimensional system, consider the following LTI system,

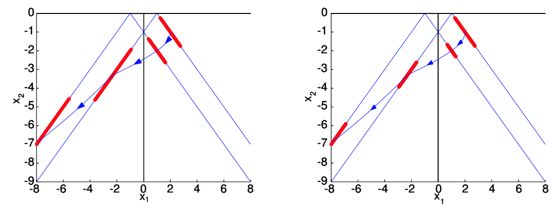

(a) Upper bounds (b) Lower bounds

Fig. 11. Upper and lower bounds on the reachable states on the switching surfaces are highlighted.

having state vector $x = \begin{bmatrix} x_1 & x_2 & x_3 \end{bmatrix}^T$ and inputs $u = \begin{bmatrix} u_1 & u_2 \end{bmatrix}^T$, with two non-linearities (shown in Figure 12) which give piecewise linear behaviour. The switching surfaces are parallel to the x_3 direction:

$$\dot{x} = \begin{bmatrix} 1 & 5 & 1 \\ -2 & -1 & 1 \\ 0 & 0 & 1 \end{bmatrix} x + \begin{bmatrix} -7 & -7 \\ 2 & -2 \\ 0 & 0 \end{bmatrix} u$$

$$\begin{bmatrix} y_1 \\ y_2 \end{bmatrix} = \begin{bmatrix} 1 & 0 & 0 \\ -1 & 1 & 0 \end{bmatrix} x$$

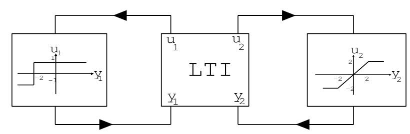

Fig. 12. LTI system with non-linearities.

Let the nominal initial state be $x_1^* = \begin{bmatrix} -4 & -2 & 1 \end{bmatrix}^T$ with an uncertainty in initial states bounded by the ellipse:

$$\delta_1^T \begin{bmatrix} 2 & 0 \\ 0 & 18 \end{bmatrix} \delta_1 = 1$$

Here, δ_1 is a vector on the initial switching surface. Using the technique we have proposed, we numerically find elliptical approximations to the reach sets on the switching surfaces. The upper bounds are shown in Figure 13 along with the nominal trajectory.

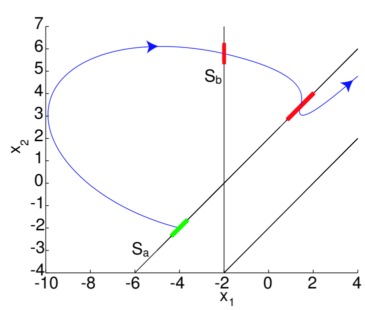

Fig. 13. Nominal trajectory and upper bounds on reach states.

Figure 11 shows the shapes of the actual reach sets in addition to the upper bound elliptical approximations on the surfaces S_a and S_b (shown in Figures 14(a) and 14(b)) and the lower bound approximations (show in Figures 14(c) and 14(d)). As can be seen, the actual reach sets are not elliptical and can only be approximated by the ellipses. The degree of the approximation ultimately depends on the shape of the actual reach set.

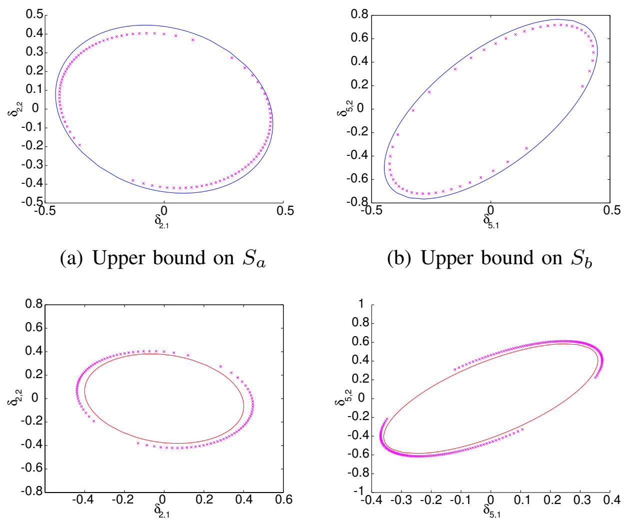

(a) Upper bound on S_a (b) Upper bound on S_b

(c) Lower bound on S_a (d) Lower bound on S_b

Fig. 14. Approximations on switching surfaces.

X. Conclusions and Future Work

A new method of finding approximations to the reach set on an arrival switching surface, given an initial start set on a departure switching surface for a general continuous-time piecewise linear system has been introduced and demonstrated. Since the system is piecewise linear, the reachable regions within each cell may be found by numerical integration and through the use of standard, well documented methods. What we have gained from this analysis is a bound on the set on a switching surface to which an initial set of points can map. This bound acts as a starting set for the next map, thus allowing us to compute reachable regions for the linear cell which the trajectories enter next. We have seen that the method is exact for two-dimensional systems, but conservative for higher order systems where the reach set cannot be bounded exactly by an ellipsoid.

The method we have described relies on our ability to solve linear matrix inequalities. The complexity of this problem is such that the LMI can be solved in polynomial time. For low order systems, computing the reachable region point by point may be possible, but it becomes computationally intractable as the degree of the system rises, hence the advantage of the method introduced here.

This analysis considered continuous-time piecewise linear systems with uncertainties in the starting set. It would be interesting to extend this to PLS with uncertainties in the shapes and positions of the switching surfaces or even the dynamics of the individual cells. This analysis may also be extended to find reachability information for systems that have piecewise behaviour that is not necessarily linear. Such systems, however, would need to have dynamics in each cell that can be described as almost linear or which can be approximated to a linear system.

Appendix I

The development with time of the state of a system, x, is given by the relation:

$$x_1 = e^{At}x_0 + \int_0^t e^{A(t-\tau)}Bd\tau$$

Since $x_0 = x_0^* + \Delta_0$ and $x_1 = x_1^* + \Delta_1$, this is equal to:

$$x_1^* + \Delta_1 = e^{At}\Delta_0 + e^{At}x_0^* + e^{At}A^{-1}B - A^{-1}B$$

Rearranging for Δ_0:

$$\Delta_0 = e^{-At}\left(x_1^* + \Delta_1 - e^{At}x_0^* - e^{At}A^{-1}B + A^{-1}B\right)$$

We know that $C_0\Delta_0 = 0$ and $C_0x_0^* = d_0$. Pre-multiplying by C_0 and rearranging yields:

$$\frac{C_0e^{-At}\Delta_1}{d_0 + C_0A^{-1}B - C_0e^{-At}A^{-1}B - C_0e^{-At}x_1^*} = 1$$

If we let:

$$v(t) = \frac{C_0e^{-At}}{d_0 + C_0A^{-1}B - C_0e^{-At}A^{-1}B - C_0e^{-At}x_1^*}$$

then we can write $v(t)\Delta_1 = 1$. We can also write:

$$J(t) = e^{-At} + \left(e^{-At}x_1^* - x_0^* - A^{-1}B + e^{-At}A^{-1}B\right)v(t)$$

Hence we obtain the impact map: $\Delta_0 = J(t)\Delta_1$.

References

[1] A.B. Kurzhanski, P. Varaiya "On Ellipsoidal Techniques for Reachability Analysis. Part I: External Approximations," Optimisation Methods and Software, Vol. 17, pp 177-206.

[2] S.V. Rakovic, E.C. Kerrigan, D.Q. Mayne, "Reachability computations for constrained discrete-time systems with state- and input-dependent disturbances," Proc. 42nd IEEE CDC, December 2003.

[3] E.C. Kerrigan, J. Lygeros, J.M. Maciejowski, "A Geometric Approach to Reachability Computations for Constrained Discrete-Time Systems." Proc. 15th IFAC World Congress on Automatic Control, Barcelona, Spain, July 2002.

[4] J.M. Gonçalves, Alexandre Megretski and Munther Dahleh. "Global Analysis of Piecewise Linear Systems Using Impact Maps and Quadratic Surface Lyapunov Functions." IEEE Transactions on Automatic Control, 48(12):2089-2106, December 2003.

[5] S. Boyd, L. El Ghaoui, Eric Feron, and V. Balakrishnan. "Linear Matrix Inequalities in System and Control Theory." SIAM, Philadelphia, 1994.

[6] J.M. Gonçalves, "Regions of Stability for Limit Cycle Oscillations via Piecewise Linear Systems," IEEE CDC, Maui, Hawaii, December 2003.